Agricultural and Forest Meteorology, 57 (1992) 281–295
Elsevier Science Publishers B.V., Amsterdam

A re-examination of the integrated horizontal flux method for estimating volatilisation from circular plots

J.D. Wilson and W.K.N. Shum
University of Alberta, Edmonton, Alta. T6G 2H4, Canada

(Received 11 February 1991; revision accepted 23 July 1991)

ABSTRACT

Wilson, J.D. and Shum, W.K.N., 1992. A re-examination of the integrated horizontal flux method for estimating volatilisation from circular plots. Agric. For. Meteorol., 57: 281–295.

Integrated horizontal flux (IHF) experiments determine the rate of volatilisation of pesticides, ammonia etc. from small circular plots to the atmosphere. To examine their accuracy, we have simulated IHF experiments by calculating the trajectories of many gaseous particles. We show that the IHF method, which requires measurements only of mean concentrations and mean cup wind speeds at several heights above the centre of the plot, estimates the rate of emission Q_0 (the ground-to-atmosphere mass flux density) to within about 20%, provided the radius R exceeds 20 m and the surface roughness length z_0 of the source plot does not exceed 0.1 m. Since a large portion of the horizontal flux to be measured occurs well below about $R/20$, we conclude that where it is practical, the IHF method is acceptably accurate.

INTRODUCTION

Many environmental chemical cycles involve emission of a gas from the ground to the atmosphere. Anthropogenic examples are the volatilisation of pesticides, and of ammonia derived from fertilisers. This paper will examine the validity of the 'integrated horizontal flux' (IHF) method for determining the emission rate from small circular field plots, a technique introduced by Beauchamp et al. (1978) and subsequently used by, among others, Brunke et al. (1988), Gordon et al. (1988), Majewski et al. (1989) and Van der Molen et al. (1990).

Considering, for the moment, the general case (rather than a small circular source area), what is required is a determination of the mass flux density Q_0 (kg m^{-2} s^{-1}) of the gas in the vertical (z) direction. Because this is a turbulent flux, accomplished by the rapidly fluctuating vertical velocity (w), it is difficult to measure. Eddy correlation methods (Kaimal, 1975) can be used, but require a fast-response concentration sensor and a sufficient upstream

fetch to permit placing the instruments at a practical height. (Businger and Oncley (1990) have introduced an empirical method based on conditional sampling that relaxes the need for a fast concentration sensor.) Present sonic anemometers for the vertical velocity impose a path-averaging length of about 10 cm and therefore fail to resolve small eddies contributing to the vertical transport below approximately 2 m. A traditional estimate of the fetch required to render the vertical flux negligibly divergent between ground and height z is $100z$ and Leclerc et al. (1990) have shown that in stable stratification this is a gross underestimation. So we can estimate that the required fetch for measurement of the vertical flux is at least 200 m, and much longer if we wish to extend the measurements through conditions of stable stratification (i.e. overnight).

A similar fetch requirement attends gradient methods, which determine Q_0 from the vertical gradient in the mean concentration of the species of interest. Such methods also require the accurate determination of small mean differences in concentration (in the presence of continuous turbulent fluctuation about the mean), an especially challenging type of measurement.

In some cases it is valuable to determine the rate of release Q_0 from plots so small (typical dimension < 100 m, say) as to render the eddy-correlation or gradient methods impractical. An example from the sphere of agronomy is

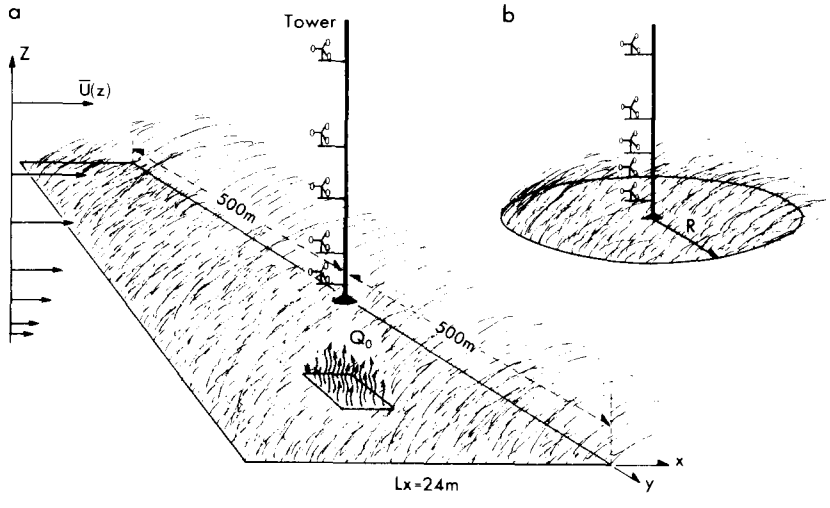

Fig. 1. Illustrating IHF methods for estimating the rate of emission Q_0 (kg m^{-2} s^{-1}) of a gas from ground to atmosphere. (a) The stripwise integrated horizontal flux (SIHF) method for a long strip of land lying across the wind. The tower at the downstream edge detects (in principle) the time-average total mass flux (kg s^{-1}) off the strip, whence with the aid of a mass-balance equation may be determined the emission rate. (b) The circular plot method is more practical (smaller plot, unaffected by wind direction) but the mass-balance equation employed (to infer source strength Q_0 from mean windspeed and concentration profiles on the tower) is not exact.

the measurement of ammonia volatilisation from small field plots, amongst which irrigation and fertiliser treatments differ. Small plot techniques will not always be sufficient, for the surface flux density Q_0 is not in general independent of the plot size. To take an obvious example, the rate of evaporation from an oasis decreases with distance from the leading edge, because of reduction in the saturation deficit as the atmospheric accumulates vapour, so the spatially-averaged vapour flux density E_0 decreases with increasing size of the oasis. However, with appropriate allowance for the sensitivity of Q_0 to the scale of the source plot, small plot experiments are useful.

Small plot techniques depend on the truth of the aphorism that "what goes up must blow away". Denmead et al. (1977) measured the rate of ammonia emission from a rectangular plot (Fig. 1a) extending $L_y = 1$ km in the crosswind (y) direction and $L_x = 24$ m in the alongwind (x) direction. A single tower supporting an array of concentration sensors and anemometers was placed at the downwind edge of the field to estimate the total mass flux of ammonia (kg s^{-1} m^{-1} of crosswind distance) blowing off the source area. For such a plot, an exact expression of mass conservation (allowing the possibility that the time-average source strength is not independent of position) is given by the equation:

$$\int_{x=0}^{L_x} Q_0 \, dx = \int_{z=0}^{\infty} \overline{uc} \, dz \tag{1}$$

where u is the velocity in the alongwind direction, c is the instantaneous concentration, and the overbar denotes a time average (over, say, 15 or 30 min).

The mean alongwind flux may be decomposed

$$\overline{uc} = \bar{u}\,\bar{c} + \overline{u'c'} \tag{2}$$

The second term on the right, the covariance of the instantaneous fluctuations u' and c' from their respective mean values, is difficult to measure. It is often assumed to be small compared with the first term; there is no general justification for this assumption, and various authors have found the turbulent flux to be sizeable (greater than 10% of the flux due to the mean flow) in some situations. Be that as it may, Denmead et al. (1977) determined mean concentration $\bar{c}$ and the mean cup windspeed:

$$\bar{s} = \overline{\sqrt{(u^2+v^2)}} \approx \bar{u}\left(1 + \frac{\overline{u'^2} + \overline{v'^2}}{2u^2}\right) \tag{3}$$

at several heights and estimated the source strength as

$$Q_0 = \frac{1}{L_x} \int_{z=0}^{\infty} \bar{s}\,\bar{c} \, dz \tag{4}$$

This we will term the 'stripwise integrated horizontal flux' (SIHF) method.

An IHF method for small circular plots (Fig. 1b), introduced by Beauchamp et al. (1978), is based on the expectation that at the centre of a plot of radius R

$$\frac{1}{Q_0 R}\int_{z=0}^{\infty} \bar{s}(z)\,\bar{c}(z)\,\mathrm{d}z \approx 1 \tag{5}$$

This expectation, the justification of which is the point of our paper, arises if we assume trajectories of elements of the emitted gas exhibit negligible lateral meandering. Under that restriction, material measured at the tower has arrived by travelling in a plane, and at any instant it is as if our detectors at the centre of the plot were actually situated a distance R from the leading edge of a source plot of infinite crosswind extent. Thus eqn. (5) proposes an effectively two-dimensional symmetry to the dispersion from a circular plot. The IHF method uses eqn. (5) to estimate Q_0, by measuring $\bar{s}$ and $\bar{c}$ at several heights to approximate the required integral.

In this paper we support the validity of eqn. (5) by carrying out a numerical imitation of IHF experiments. We calculate the trajectories of a large number of fluid particles emanating from representative sectors of the plot; only those particles which pass through a detection cylinder at the axis of the plot contribute to the observed concentration.

The exactness of eqn. (1) for the geometry to which it applies has resulted in a temptation to base an IHF method for circular plots upon integration of the total quasi-flux $\overline{sc}$. We call $\overline{sc}$ a quasi-flux because a true flux is a vector (or a component thereof) and has an unambiguous direction, whereas $\overline{sc}$, and for that matter $\bar{s}\,\bar{c}$, being fluxes with no meaningful direction, do not have a clear interpretation. In fact, there is no reason to expect either

$$A=\frac{1}{Q_0 R}\int_0^{\infty} \bar{s}(z)\,\bar{c}(z)\,\mathrm{d}z \quad \text{or} \quad A'=\frac{1}{Q_0 R}\int_0^{\infty} \overline{sc}(z)\,\mathrm{d}z$$

measured at the axis of a circular plot to be exactly unity, nor is it certain that A' is closer to unity than A. Few IHF experiments to date have measured the flux $\overline{sc}$; its determination is complicated by the need for fast concentration and speed sensors, or a directly flux-proportional sampler such as described and used (for ammonia) by Leuning et al. (1985). In this paper, we examine only the fidelity of eqn. (5), envisaging that most users will prefer to base their IHF technique on the simpler measurements $\bar{s}$ and $\bar{c}$.

Gordon et al. (1988) reported that three- and two-dimensional Lagrangian stochastic (LS) models predict different profiles at the centre of a plot of radius $R=3.5$m. Their LS model is not fully documented and it is not clear

whether they included the fluctuation u' in alongwind velocity. We concentrate here, not on the difference between two- and three-dimensional predictions but upon whether, according to the best imitation of three-dimensional atmospheric trajectories which can be carried out with our present knowledge, eqn. (5) applied to an IHF experiment will give an accurate estimate of the source strength.

In the following section we detail the 'Lagrangian stochastic' or 'random flight' model we have used for our calculations, and our specification of the atmospheric state (which we allow to vary from very unstable through neutral to very stable).

LAGRANGIAN STOCHASTIC MODEL

The random flight of each particle is calculated in a sequence of short timesteps $\mathrm{d}t$, during each of which the particle moves by distances: $\mathrm{d}x=[\bar{u}(z)+u]\,\mathrm{d}t$, $\mathrm{d}y=v\,\mathrm{d}t$, $\mathrm{d}z=w\,\mathrm{d}t$. Here $\bar{u}(z)$ is the mean alongwind velocity at the present height of the particle and u, v and w are the turbulent velocities (henceforth we will drop the prime on fluctuations), for which a model is required.

We have used a heuristic generalisation to three dimensions of a one-dimensional model given originally by Wilson et al. (1983a) and subsequently proven satisfactory by Thomson (1984, 1987)

$$\mathrm{d}w=-\frac{\mathrm{d}t}{\tau_{\mathrm{L}}}w+\frac{1}{2}\frac{\partial\sigma_w^2}{\partial z}\left(1+\frac{w^2}{\sigma_w^2}\right)\mathrm{d}t+\sqrt{\left(\frac{2\sigma_w^2}{\tau_{\mathrm{L}}}\right)}\mathrm{d}\xi_w \tag{6}$$

$$\mathrm{d}z=w\,\mathrm{d}t \tag{7}$$

$$\mathrm{d}t=\mu\tau_{\mathrm{L}}(z) \tag{8}$$

where $\tau_{\mathrm{L}}(z)$ is the Lagrangian timescale, σ_w is the standard deviation of the vertical velocity, $\mathrm{d}\xi_w$ is a random variate chosen from a Gaussian distribution with mean zero and variance $\mathrm{d}t$, and μ is required to satisfy $\mu\ll 1$. This is a suitable model for the vertical velocity of a neutrally-buoyant particle in inhomogeneous turbulence, provided the Eulerian velocity has a Gaussian distribution. A general specification for the (actually non-Gaussian) surface-layer probability density function and a consistent trajectory model remain to be formulated.

Wilson et al. (1983a) gave the model (eqns. (6)–(8)) in the form of a Markov chain for the ratio $q_w=w/\sigma_w$ of the vertical velocity to its local standard deviation. Our generalisation is

$$q_u^{(t+\mathrm{d}t)}=\alpha\,q_u^{(t)}+\beta[c_u r_u^{(t+\mathrm{d}t)}+c_w r_w^{(t+\mathrm{d}t)}] \tag{9}$$

$$q_v^{(t+\mathrm{d}t)}=\alpha\,q_v^{(t)}+\beta\,r_v^{(t+\mathrm{d}t)} \tag{10}$$

$$q_w^{(t+\mathrm{d}t)} = \alpha\, q_w^{(t)} + \beta\, r_w^{(t+\mathrm{d}t)} + \gamma\, \tau_\mathrm{L} \frac{\partial \sigma_w}{\partial z} \tag{11}$$

where

$$\alpha = 1 - \frac{\mathrm{d}t}{\tau_\mathrm{L}},\ \beta = \sqrt{(1-\alpha^2)},\ \gamma = 1-\alpha \tag{12}$$

The velocity fluctuations are obtained by multiplying the dimensionless q values by the appropriate velocity standard deviations

$$u = q_u \sigma_u \qquad v = q_v \sigma_v \qquad w = q_w \sigma_w \tag{13}$$

The r values are mutually independent random Gaussian variables, each having mean zero, unit variance and vanishing autocovariance $<r^{(t)} r^{(t+\mathrm{d}t)}>$ for non-zero dt. The q values each have unit variance and are independently initialised upon release of the particle as: $q_u^{(0)} = r_u$ etc. The appearance of r_w in the Markov chain for q_u gives rise to the correct kinematic shear stress $<uw> = -u_*^2$ provided

$$c_w = -\frac{u_*^2}{\sigma_u \sigma_w},\ c_u = \sqrt{(1-c_w^2)} \tag{14}$$

Should a particle descend below the roughness length z_0 it is 'bounced', i.e. $z \leftarrow 2z_0 - z$ and $q_w \leftarrow -q_w$.

It will be noted that we impose the same timescale $\tau_\mathrm{L}(z)$ upon all three turbulent velocity components. This we believe to be acceptable for the present purpose. It is the high frequency end of the horizontal velocity spectra that governs meandering; power at low frequency in the spectrum S_v of v merely causes the wind to prefer blowing from a particular direction over intervals compared to the typical time taken for an emitted particle to blow across the plot. At frequencies near the spectral peak f_max in w (where the energy in w resides), i.e. at frequencies well above the energy-containing region of the horizontal spectra, the horizontal and vertical Eulerian velocity spectra have similar magnitude and variation with height and stability (Kaimal, 1978). So we expect that, in the high frequency region causing meandering, the Lagrangian spectra will be at least similar, thus justifying the use of the same timescale for each direction of motion.

Specification of the atmospheric surface-layer

Mean windspeed

The variation of the mean wind with height may be written

$$\bar{u}(z) = \frac{u_*}{k}\left[\ln\frac{z}{z_0} - \psi\left(\frac{z}{L}\right) + \psi\left(\frac{z_0}{L}\right)\right] \tag{15}$$

where u_* is the friction velocity and $k=0.4$ is von Karman's constant. In unstable stratification (Monin–Obukhov length $L<0$) we used (Businger, 1973)

$$\psi\left(\frac{z}{L}\right)=2\ln\left(\frac{1+\phi}{2}\right)+\ln\left(\frac{1+\phi^2}{2}\right)-2\tan^{-1}\phi+\frac{\pi}{2} \tag{16}$$

$$\phi\left(\frac{z}{L}\right)=\left(1-15\frac{z}{L}\right)^{1/4} \tag{17}$$

and in stable stratification (Businger, 1973)

$$\psi\left(\frac{z}{L}\right)=-5\frac{z}{L} \tag{18}$$

Turbulent velocity standard deviations

According to Panofsky et al. (1975) the horizontal velocity standard deviations σ_u and σ_v in the unstably-stratified surface-layer obey the formula

$$\sigma_{u,v}=u_*[12+0.5(\delta/-L)]^{1/3} \tag{19}$$

where δ is the depth of the planetary boundary layer (PBL). Panofsky and Dutton (1984) note that under stable stratification the ratios $\sigma_{u,v}/u_*$ retain values appropriate to neutral stratification (about 2), except for very large z/L, where they become large and unpredictable.

Because we use a single timescale for all three velocity components, we have chosen to use $\sigma_u=\sigma_v=2.0u_*$ for all L. Our reasoning, which is admittedly qualitative, is as follows. Much of the power in u and v lies in the 'energy-containing region' at frequencies far lower than the region of the spectral peak in w (Kaimal, 1978). When L is small and negative, i.e. in very unstable stratification, $\sigma_{u,v}$ are much larger than $2u_*$, e.g. being approximately $6u_*$ when $\delta=2000$ m and $L=-5$ m. However, much of this additional power lies at low frequency and will not cause meandering of trajectories across a small plot. If we allow $\sigma_{u,v}$ to be increased in the LS model without altering the timescale (which, as discussed above, is set equal to the timescale for the vertical velocity and therefore represents the high frequency end of the u,v spectra) we will cause a spurious increase in the meandering of trajectories. In fact, (to reiterate, because much of the power in u and v lies at low frequency), it may be that even using $\sigma_u=\sigma_v=2.0u_*$ we overestimate meandering; if so, errors in the IHF method because of three-dimensionality of trajectories are even smaller than we have concluded here.

For the standard deviation of the vertical velocity we use (Panofsky et al., 1975)

$$\sigma_w=1.25u_* \qquad L>0 \tag{20}$$

$$\sigma_w=[1.6+2.9\,(-z/L)^{2/3}]^{1/2} \qquad L<0 \tag{21}$$

Lagrangian timescale

By comparing the prediction of a Lagrangian stochastic model with experimental data, Wilson et al. (1981) recommended, for the timescale τ_L for the vertical velocity, the choice $\tau_L = l/\sigma_w$ where the length scale l is given by the formulae

$$l = 0.5z\left(1 - 6\frac{z}{L}\right)^{1/4} \qquad L < 0 \tag{22}$$

$$l = 0.5z\left(1 + 5\frac{z}{L}\right)^{-1} \qquad L > 0 \tag{23}$$

For situations in which σ_w is height-dependent, the model of Wilson et al. differs very slightly from the present formulation. Rather than accepting a priori the above choice for the timescale in unstable stratification, we performed random flight simulations with the 1-dimensional model (eqns. (6)–(8)) and

$$l = 0.5z\left(1 - a\frac{z}{L}\right)^{-n} \qquad L < 0 \tag{24}$$

Best agreement with the unstable Project Prairie Grass experiments (Barad, 1958) was obtained, as in the earlier model of Wilson et al. (1981), with $a = 6$, $n = 1/4$.

Calculation of the mean concentration

The source plot is subdivided radially (by $n = 60$) and angularly (by $m = 72$) into sectors of area $\mathrm{d}A_{nm}$. N_p particles are released at $z = z_0$ (sequentially and independently) from the centres of each sector. Given our very fine subdivision of the plot we assumed the choice of release position within each source element to be insignificant. Each particle is tracked until it has passed at least 3 m downstream from plot centre (this criterion was found sufficient to ensure very low probability of the particle returning to make a further contribution to the mean concentration).

The 'detection cylinder' lies along the vertical axis at the plot centre. It has radius $r_c \ll R$ (in practice $< 0.02R$) and is subdivided along the vertical (index J) into subcylinders of depth Δz_c and volume $\Delta V = \pi r_c^2 \Delta z_c$ to resolve the vertical mean concentration gradient. Our choice of Δz_c varied in the range 0.005–0.2 m with plot radius and stability, never exceeding $R/50$. Each time a particle from sector nm spends time δt within subcylinder J, a weighted residence time accumulator $T(J)$ is incremented by amount $\delta t\ \mathrm{d}A_{nm}$, i.e. $T(J) = \Sigma\ \delta t\ \mathrm{d}A_{nm}$. Mean concentration $\bar{c}(J)$ in the Jth subcylinder is calculated, after all particles from all source sectors have flown, as

$$\bar{c}(J) = Q_0 T(J) / (\Delta V N_P) \tag{25}$$

Test of IHF method

In order to test eqn. (5), the mean cup windspeed $\bar{s}(J)$ is calculated at the midpoint of each detection cylinder as

$$\bar{s}(J) = \frac{1}{N} \sum_{i=1}^{N} \sqrt{[(\bar{u}(J) + u_i)^2 + v_i^2]} \tag{26}$$

where $\bar{u}(J)$ is the mean alongwind velocity at that height and u_i, v_i are random fluctuations, chosen at random from the Gaussian distribution with zero mean and the appropriate standard deviation. The number of samples, N, is sufficient to reduce the standard error in $\bar{s}(J)$ to below 1%.

The accuracy A_{IHF} of the simulated IHF experiment is defined as

$$A_{\mathrm{IHF}} = \frac{\sum_{\text{all } J} \bar{s}(J)\, \bar{c}(J)\, \Delta z_c}{Q_0 R} \tag{27}$$

RESULTS AND DISCUSSION

We simulated IHF experiments under atmospheric conditions of extreme stability ($L = +5$ m), neutrality ($|L| = \infty$) and extreme instability ($L = -5$ m). Two surface roughness values were investigated, $z_0 = 0.01$ m, 0.1 m. It should be noted that if z_0 is of order 0.1 m the IHF method is probably hard to implement (except for very large R), because much of the lateral flux will occur within the vegetation where the cup windspeed is low and therefore hard to measure.

Our results are presented in Table 1 and Fig. 2. We draw the following two conclusions.

(1) The accuracy of the IHF method deteriorates with decreasing plot radius, rapidly so for large roughness length ($z_0 = 0.1$ m) and $R < 20$ m.

(2) For a given radius, the accuracy of the IHF method deteriorates as roughness length z_0 increases.

Both these limitations of the IHF method can be attributed to the fact that as the ratio σ_v / U of typical lateral fluctuation velocity to representative advection velocity U increases, more meandering of the particle trajectories can be expected (i.e. greater departure from the ideal condition of motion in a single plane). We illustrate using the neutral case

$$\frac{\bar{u}(z)}{u_*} = \frac{1}{k_v} \ln \frac{z}{z_0}, \quad \frac{\sigma_v}{u_*} \approx 2$$

TABLE 1

Tabulation of the accuracy A_{IHF} of simulated IHF experiments over a range of conditions (in brackets, the standard error of the estimate)

	R (m)	A_{IHF}		
		Stable ($L_{MO}=5$ m)	Neutral ($L_{MO}=\infty$)	Unstable ($L_{MO}=-5$ m)
$z_0=0.01$ m	2.5	1.13 (0.02)	1.18 (0.03)	1.14 (0.02)
	5	1.11 (0.02)	1.14 (0.01)	1.13 (0.02)
	10	1.10 (0.02)	1.08 (0.03)	1.10 (0.02)
	20	1.03 (0.03)	1.07 (0.03)	1.07[1] (0.04)
	50	1.00 (0.02)	1.05 (0.04)	1.04 (0.04)
	100	1.02 (0.03)	1.05 (0.04)	1.03 (0.06)
$z_0=0.1$ m	2.5	1.35 (0.03)	1.48 (0.03)	1.52 (0.03)
	5	1.28 (0.03)	1.34 (0.02)	1.37 (0.02)
	10	1.20 (0.02)	1.29 (0.02)	1.28 (0.02)
	20	1.10 (0.03)	1.19 (0.03)	1.21 (0.03)
	50	1.09 (0.03)	1.13 (0.04)	1.16 (0.03)
	100	1.07 (0.03)	1.13 (0.03)	1.13 (0.03)

[1]If $\sigma_{u,v}$ are permitted to increase with increasing instability according to eqn. (19), we obtain here the value $A_{IHF}=1.16$ (0.06).

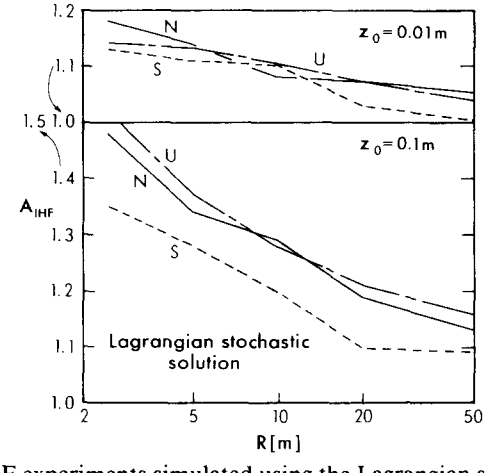

Fig. 2. Accuracy of IHF experiments simulated using the Lagrangian stochastic model, for two values of surface roughness z_0 and over a range in plot radius. Stratification: stable, S (---), $L_{MO}=5$ m; neutral, N (——), $L_{MO}=\infty$; unstable, U (— —), $L_{MO}=-5$ m.

Deterioration of the IHF method with decreasing R is a result of the confinement of trajectories to lower heights, with consequently exaggerated σ_v/U. For example, let $z_0=0.01$ m and consider a typical advection height to be $R/200$. Then:

(a) $R=2$ m implies $U\approx 0$, hence $\sigma_v/U\approx\infty$. Under these conditions trajectories will look (from above) like tangled string, or the antics of a fly over a plate of meat.

(b) $R=50$ implies $U/u_*\approx 8$ and $\sigma_v/U\approx 0.25$. We would expect much less meandering and therefore greater accuracy of the IHF experiment.

Deterioration with increasing roughness length has the same explanation: as z_0 increases, U is decreased without change in σ_v, amplifying σ_v/U. We will now show that this effect is predicted by a simple analytical model.

A simple analytical simulation of the IHF experiment

It is not hard to construct a simple analytical model which will demonstrate these effects. Assume an alongwind (x) speed U which is constant in time and space, and random cross-stream fluctuations having standard deviations $\sigma_{v,w}$ independent of position (homogeneous turbulence). The mean cup windspeed at any height is, using a binomial expansion

$$\bar{s}=\overline{\sqrt{(U^2+v^2)}}\approx U\left(1+\frac{\sigma_v^2}{2\,U^2}\right) \tag{28}$$

We can express the mean concentration at any height z on the axis of the plot as

$$\bar{c}=\int \mathrm{d}c$$

where $\mathrm{d}c$ is the contribution from the infinitesmal plot area $r\cdot\mathrm{d}\phi\cdot\mathrm{d}r$ which lies distance r from the plot centre along the radius making angle ϕ with respect to the x-axis.

Assume the concentration distributions in both y and z directions are Gaussian (in the latter case folded about $z=0$ to account for the reflecting ground). The standard deviations σ_y, σ_z are functions of the advection time, which is controlled by the distance $r\cos\phi$ along the x-axis to the source element. Then we may express $\mathrm{d}c$ as

$$\mathrm{d}c(r,\phi)=2\frac{Q_0 r\,\mathrm{d}\phi\,\mathrm{d}r}{2\pi\,\sigma_y\sigma_z U}\exp\left(-\frac{\mathrm{y}^2}{2\,\sigma_y^2}\right)\exp\left(-\frac{z^2}{2\sigma_z^2}\right) \tag{29}$$

where $y=r\sin\phi$ is the lateral offset of the source element from the x-axis through $r=0$. Equation (29) is readily shown to satisfy the appropriate advection-diffusion equation expressing mass conservation (in this simplified flow) and the necessary boundary conditions for a continuous point source.

Because we will be integrating eqn. (29) with respect to z, we will not need to know σ_z. We use Taylor's (1921) classical solution for the crosswind spread as a function of the alongwind fetch $r\cos\phi$; assuming an exponential Lagran-

gian autocorrelation function with Lagrangian timescale τ_v for the lateral particle velocity v, this is

$$\sigma_y^2 = 2\sigma_v^2\{t\tau_v - \tau_v^2[1-\exp(-t/\tau_v)]\} \tag{30}$$

where t is the advection time $t = r\cos\phi/U$.

It is a simple matter to show that, according to this model, the accuracy of the IHF method is

$$A_{\mathrm{IHF}} = \int_{z=0}^{\infty} \frac{\bar{s}\,\bar{c}}{Q_0 R}\mathrm{d}z = 2\frac{\bar{s}}{U}\int_{r=0}^{R}\int_{\phi=0}^{\frac{\pi}{2}} \frac{r\,\mathrm{d}\phi\,\mathrm{d}r}{\sqrt{(2\pi)}\sigma_y}\exp[-y^2/(2\sigma_y^2)] \tag{31}$$

(where y and σ_y depend upon r and ϕ). The free dimensionless factors determining A_{IHF} are: (1) σ_v/U, typical lateral to mean alongwind velocity ratio; (2) $\sigma_v\tau_v/R$, ratio of length scale of lateral wind fluctuations to plot radius.

Equation (31) has been solved numerically using increments $\mathrm{d}\phi = 2°$, $\mathrm{d}r = 0{\cdot}02R$. All solutions yielded $A_{\mathrm{IHF}} \geq 1$. Figure 3 shows the variation in A_{IHF} versus σ_v/U for several values of $\sigma_v\tau_v/R$. As in our much more realistic three-dimensional Lagrangian stochastic simulation, accuracy deteriorates as σ_v/U increases. If the impact of reducing the plot size is investigated by increasing $\sigma_v\tau_v/R$ while holding σ_v/U constant, a result converse to that of the LS model is obtained: better accuracy at smaller plot size. However, this is a spurious result which does not represent reality – we know that as R decreases the shallower plume encounters smaller advection velocity and therefore larger effective σ_v/U.

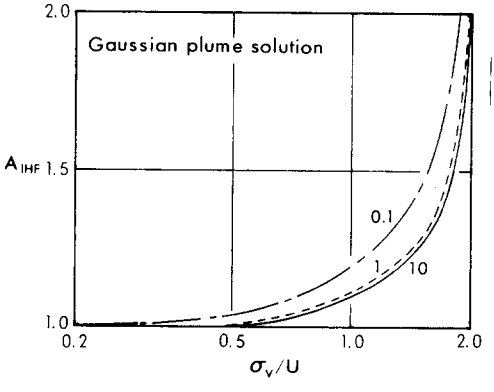

Fig. 3. Accuracy of IHF experiments in hypothetical homogeneous turbulence (no shear in the mean wind U) as a function of the ratio σ_v/U of lateral velocity standard deviation to advection velocity and the ratio $\sigma_v\tau_v/R$ of a meandering length scale to plot radius.

CONCLUSION

Our results indicate that the IHF method will yield emission rates Q_0 accurate to within about 20% or better, for plot radii 20 m $\leq R \leq$ 100 m and for roughness lengths z_0 less than about 0.1 m. If the roughness length is small, say 0.01 m, plot sizes smaller than $R = 20$ m are acceptable vis-à-vis the validity of eqn. (5) but they may be impractical because the measurement heights descend with diminishing plot size. On first thought one might have expected an improvement in the IHF method as plot size decreases (shorter distances from source to detector). However, the opposite is the case, because for smaller plots the plume is confined closer to ground where the mean component of the horizontal velocity is smaller.

Is 20% accuracy sufficient? Almost certainly so, because field IHF experiments are susceptible to known or unsuspected departures from the ideal, such as non-uniform surface condition, inhomogeneous source strength, measurement error in windspeed and concentration, imperfectly circular geometry and extrapolation error in estimation of the vertical integral in eqn. (5). It is not useful – in fact probably meaningless – to require a theory to be more accurate than the experiments which could test it. Therefore one should not feel obliged to consider the IHF technique inaccurate because it may be in error by the order of 20%.

The validity of our finding rests with the accuracy of our calculated trajectories. Our Lagrangian stochastic model does not incorporate the impact of, e.g. non-zero skewness and kurtosis in the velocities, and our conclusions should probably be scrutinised when a more general model becomes available. However, we suspect a more crucial point, given that we are most concerned with meandering, is our manner of incorporating u and v. In our choices for the variance and timescale of these velocity fluctuations we have been reduced to qualitative arguments and we cannot even suggest how the implementation of u, v might by formalised. Because there is a wide distribution of travel times from release to plot centre (even for fixed R, L, and z_0), specification of the pertinent part (that causing meandering) of the spectra of u and v is difficult.

Finally, a word about the theoretical profile shape (TPS) method, introduced by Wilson et al. (1982), and tested by Wilson et al. (1983b) and subsequently others (e.g. Majewski et al., 1989). Briefly, the TPS method reduces the experimental input required to determine the emission rate Q_0 to measurement of mean windspeed $\bar{s}$ and mean concentration $\bar{c}$ at a single (but not arbitrary) height ZINST, chosen in such a way that the sensitivity of the ratio $\bar{s}\,\bar{c}/Q_0$ to stability (L) is weak. The penalty for ignoring the influence of stratification is insignificant relative to likely errors in the (instrumentally) more demanding IHF method. The simplification of the TPS relative to the IHF method is achieved by a calibrating determination of the ratio $\bar{s}\,\bar{c}/Q_0$

according to a model of turbulent dispersion applied to the given geometry and flow. Equally, one could calibrate the ratio $\overline{sc}/Q_0$, but there is little point, as that would require usage of more-complex instrumentation. Our point in mentioning the TPS method (which is in common use) is that the question addressed in this paper (the validity of eqn. (5) does not bear on the correctness of the TPS method. Even if eqn. (5) were wildly incorrect, the TPS method, provided it is correctly calibrated, stands. Wilson et al. (1982) calibrated the TPS method for two plot sizes using a two-dimensional LS model. Since the predictions of two- and three-dimensional simulations for the profiles at the plot centre are not identical (Gordon et al., 1988), caution suggests a comprehensive re-calibration of the TPS method using a sound and well-documented three-dimensional model. We believe, however, that the error inherent in using a TPS method based on the earlier-provided two-dimensional calibration cannot be large. Evidence for this is the good agreement of the (herein verified) IHF method and the TPS method (two-dimension calibration) demonstrated by Wilson et al. (1983b).

ACKNOWLEDGEMENTS

The authors are grateful for the support of the Natural Sciences and Engineering Research Council of Canada, in the form of an Operating Grant (J.D. Wilson) and an Undergraduate Research Award (W.K.N. Shum). We thank Dr. T. Flesch for his helpful review of the manuscript.

REFERENCES

Barad, M.L., 1958. Project Prairie Grass, a Field Program in Diffusion (Vol. II). Geophysical Research Papers No. 59, Air Force Cambridge Research Center TR-58-235(II), National Technical Information Service NTIS AD-152573.

Beauchamp, E.G., Kidd, G.E. and Thurtell, G.W., 1978. Ammonia volatilisation from sewage sludge applied in the field. J. Environ. Qual., 7: 141–146.

Brunke, R., Alvo, P., Schuepp, P. and Gordon, R., 1988. Effect of meteorological parameters on ammonia loss from manure in the field. J. Environ. Qual., 17: 431–436.

Businger, J.A., 1973. Turbulent transfer in the atmospheric surface layer. In: D.A. Haugen (Editor), Workshop on Micrometeorology. American Meteorological Society, Boston, pp. 67–100.

Businger, J.A. and Oncley, S.P., 1990. Flux measurement with conditional sampling. J. Atmos. Oceanic Tech., 7: 349–352.

Denmead, O.T., Simpson, J.R. and Freney, J.R., 1977. A direct field measurement of ammonia emission after injection of anhydrous ammonia. Soil Sci. Soc. Am. J., 41: 1001–1004.

Gordon, R., Leclerc, M.Y., Schuepp, P. and Brunke, R., 1988. Field estimates of ammonia volatilisation from swine manure by a simple micrometeorological technique. Can. J. Soil Sci., 68: 369–380.

Kaimal, J.C., 1975. Sensors and techniques for direct measurement of turbulent fluxes and profiles in the atmospheric surface layer. Atmos. Technol., 7: 7–14.

Kaimal, J.C., 1978. Horizontal velocity spectra in an unstable surface layer. J. Atmos. Sci., 35: 18–24.

Leclerc, M.Y. and Thurtell, G.W., 1990. Footprint prediction of scalar flux using a Markovian analysis. Boundary-Layer Meteorol., 52: 247–258.

Leuning, R., Freney, J.R., Denmead, O.T. and Simpson, J.R., 1985. A sampler for measuring atmospheric ammonia flux. Atmos. Environ., 19: 1117–1124.

Majewski, M.S., Glotfelty, D.E. and Seiber, J.E., 1989. A comparison of the aerodynamic and the theoretical-profile-shape methods for measuring pesticide evaporation from soil. Atmos. Environ., 23: 929–938.

Panofsky, H.A. and Dutton, J.A., 1984. Atmospheric Turbulence. Wiley Interscience, NY.

Panofsky, H.A., Tennekes, H., Lenschow, D.H. and Wyngaard, J.C., 1975. The characteristics of turbulent velocity components in the surface layer under convective conditions. Boundary-Layer Meteorol., 11: 355–361.

Taylor, G.I., 1921. Diffusion by continuous movements. Proc. London Math. Soc. Series 2, 20: 196–212.

Thomson, D.J., 1984. Random walk modelling of diffusion in inhomogeneous turbulence. Q.J.R. Meteorol. Soc., 110: 1107–1120.

Thomson, D.J., 1987. Criteria for the selection of stochastic models of particle trajectories in turbulent flows. J. Fluid Mech., 180: 529–556.

Van der Molen, J., van Faassen, H.G., Leclerc, M.Y., Vriesema, R. and Chardon, W.J., 1990. Ammonia volatilisation from arable land after application of cattle slurry. 1. Field estimates. Netherlands J. Agric. Sci., 38: 145–158.

Wilson, J.D., Thurtell, G.W. and Kidd, G.E., 1981. Numerical simulation of particle trajectories in inhomogeneous turbulence. III. Comparison of predictions with experimental data for the atmospheric surface-layer. Boundary-Layer Meteorol. 21: 295–313.

Wilson, J.D., Thurtell, G.W., Kidd, G.E. and Beauchamp, E.G., 1982. Estimation of the rate of gaseous mass transfer from a surface source plot to the atmosphere. Atmos. Environ., 16: 1861–1867.

Wilson, J.D., Legg, B.J. and Thomson, D., 1983a. Calculation of particle trajectories in the presence of a gradient in turbulent-velocity variance. Boundary-Layer Meteorol., 27: 163–169.

Wilson, J.D., Catchpoole, V.R., Denmead, O.T. and Thurtell, G.W., 1983b. Verification of a simple micrometeorological method for estimating ammonia loss after fertiliser application. Agric. Meteorol., 29: 183–189.